

EXPERIMENTAL STUDY OF GAS ABSORPTION INTO TURBULENT FALLING FILMS OF WATER AND ETHYLENE GLYCOL-WATER MIXTURES*

D. K. CHUNG and A. F. MILLS
University of California, Los Angeles, CA 90024, U.S.A.

(Received 18 September 1974 and in revised form 18 March 1975)

Abstract—Experiments are reported on the effects of liquid viscosity and interfacial shear on the liquid side mass-transfer coefficient for turbulent falling films. CO₂ gas was absorbed into a liquid film formed on the inside of a 2.05 cm ID, 1.98 m long vertical tube. The Reynolds number power dependence of the mass-transfer coefficient was found to depend markedly on viscosity. Transition from wavy laminar to turbulent flow occurred at Reynolds numbers from 1000 to 1200. With co-current gas flow a marked and linear increase in mass-transfer coefficient was found, while for counter-current gas flow the coefficient decreased.

NOMENCLATURE

- c , concentration of solute gas;
- \mathcal{D} , molecular diffusion coefficient;
- g , acceleration due to gravity;
- H , Henry's constant;
- K_L , liquid side mass-transfer coefficient;
- P , pressure;
- Re_L , film Reynolds number, $= 4\Gamma/\rho v$;
- Sc , Schmidt number, $= \nu/\mathcal{D}$;
- u , velocity;
- We , Weber number, $= \rho_b u_b^2/\sigma$;
- X , mole fraction of ethylene glycol.

Greek symbols

- Γ , mass flow rate per unit width;
- δ , film thickness;
- ν , kinematic viscosity;
- ρ , density;
- σ , surface tension;
- τ , shear stress.

Subscripts

- b , bulk value;
- g , gas phase;
- i , liquid phase at interface;
- L , liquid;
- w , tube wall;
- in, out, bulk values in inlet and outlet liquid, respectively.

Superscript

- 0, zero interfacial shear.

1. INTRODUCTION

NUMEROUS theoretical models for the prediction of gas absorption into a turbulent falling liquid film have been published; a good review of the work prior to 1969 has been given by Scriven [1]. The problem is a difficult one owing to the complexity of the turbulent mixing motion in the liquid near the liquid-gas interface, and the highly disturbed nature of this interface. Most of the models predict that the mass-transfer coefficient depends on the molecular diffusion coefficient to the one-half power, however none satisfactorily predict the dependence on film Reynolds number and liquid properties. In view of this insufficiency in the theoretical approach there is a clear need for good experimental data over a wide range of parameters; however, such data for turbulent falling films is relatively sparse. The previous experimental work is reviewed below.

1. Kamei and Oishi [2] absorbed CO₂ into water at temperatures from 8.5°C to 50°C in a long wetted wall column. The Reynolds number range was 55 to 11000. In the turbulent flow regime the data was correlated as

$$K_L \propto \mathcal{D}^{1/2} Re_L^{0.7}. \quad (1)$$

They also concluded from their data that surface tension had no effect on K_L ; however the surface tension of water varied only 9 per cent in their temperature range so that such a conclusion was hardly warranted. Kamei and Oishi also attempted some experiments with counter-current gas flow but the scatter in their data precluded any meaningful conclusion.

2. Emmert and Pigford [3] absorbed O₂ and CO₂ into water in both short and long columns. Their liquid Reynolds number was mostly in the wavy laminar regime and K_L values were several-fold higher than those predicted by laminar theory. The short range of

*This work was supported by the University of California Water Resources Center on Project No. S142, and by National Science Foundation Grant GK-40180. Computer time was supplied by the Campus Computing Network of the University of California, Los Angeles.

turbulent data precluded determination of the Reynolds number dependence, but did show a transition to turbulence at about $Re_L = 1200$. They also noted differences in K_L for absorption vs desorption but could not explain this result.

3. Davies and Warner [4] investigated the effect of surface roughness on the liquid side mass-transfer coefficients for CO_2 , H_2 and He absorbing into water flowing along an inclined plate, and found $K_L \propto \mathcal{D}^{0.52}$.

4. Lamourelle and Sandall [5] absorbed He, H_2 , O_2 and CO_2 into water at 25°C flowing on the outside wall of a long vertical column. The Reynolds number ranged from 1300 to 8300. Their data was well correlated by

$$K_L \propto \mathcal{D}^{0.537} Re_L^{0.837}. \quad (2)$$

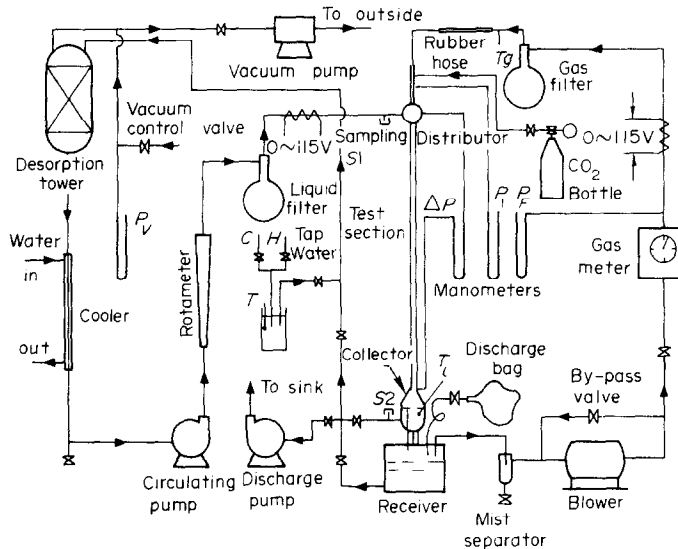


FIG. 1. Schematic of experimental apparatus.

We report here the results of an experimental study of absorption of carbon dioxide into turbulent falling films of water and ethylene glycol-water mixtures. These liquids may be characterized as having a "high" surface tension. For absorption from a stagnant gas phase seven liquids were used: tap water at three different temperatures, distilled water and three mixture ratios of ethylene glycol and water, giving a wide range of liquid kinematic viscosity. In each case the film Reynolds number range was extended into the wavy laminar regime in order to establish the transition between wavy laminar and turbulent flow. For absorption from a co-current gas flow, tap water and two ethylene glycol water mixtures were used, while for counter-current gas flow only tap water was used. The high liquid phase Schmidt numbers which prevail imply a very steep concentration profile adjacent to the interface; thus changes in the fluid mechanics in the vicinity of the interface due to interfacial shear might be expected to have a significant effect on K_L . The data presented here is of direct utility in the design of process equipment; in addition a wide data base is provided for the evaluation of theoretical analyses of transport adjacent to fluid interfaces.

2. EXPERIMENTAL APPARATUS AND PROCEDURES

2.1. Apparatus

A schematic of the experimental apparatus is shown in Fig. 1. The system comprised of two main loops, the liquid flow loop and the gas flow loop. The components of the liquid loop were: circulating pump, rotameter, activated carbon filter, absorption column, liquid receiver, desorption tower and various valves, fittings and connecting tubing. All components were of stainless steel or glass construction. A closed liquid loop was used for all liquids except tap water, in which case the water was sucked into the desorption tower and after flowing through the loop once was discharged through a pump into a sink. The components of the gas flow loop were: a gas blower, mist separator, gas

flow meter and activated carbon filter, connected by copper tubing and galvanized steel pipes.

The liquid film was formed on the inside wall of a 2.05 cm ID, 1.98 m long vertical glass tube. To obtain a uniform film thickness around the periphery, and to minimize entrance effects in both the liquid and gas flows a slot shaped distributor was carefully machined and assembled. The 1.1 mm width of the slot was close to the film thickness at the higher Reynolds numbers used. Lamourelle and Sandall [5] found that entrance effects of a similar distributor were not detectable by testing several different lengths of column. To minimize splashing where the liquid film met the liquid in the collector the liquid entrance was made in the form of a bell mouth. The liquid level in the collector was maintained constant by an overflow pipe connected between the collector and receiver. The end effect due to the increased absorption area in the collector was approximately accounted for by adding 4 cm to the actual distance (194 cm) between the distributor exit and the collector liquid level when calculating the mass-transfer coefficient.

The desorption tower comprised of a bundle of wetted wall columns and was maintained at about

Table 1. Liquid phase properties

	ρ (kg/m ³)	$\sigma \times 10^3$ (N/m)	c (kg mole/m ³ atm)	$\nu \times 10^6$ (m ² /s)	$\mathcal{D} \times 10^9$ (m ² /s)	Sc	$\nu(g\rho^3/\sigma^3)^{1/4}$ $\times 10^3$
Ethylene glycol-water mixtures at 25°C							
$X = 0.00$	997	72	0.0346	0.898	1.96	458	2.03
0.052	1015	65	0.0302	1.30	1.58	822	3.20
0.12	1036	61	0.0279	1.88	1.22	1540	4.95
0.20	1053	57.5	0.0270	2.75	1.02	2700	7.66
Tap water at various temperatures							
$T = 40^\circ\text{C}$	992	69.6	0.0240	0.661	2.8	236	1.53
25°C	997	72	0.0343	0.898	1.96	458	2.03
14°C	999	73.5	0.0472	1.171	1.44	813	2.61

5 cm Hg absolute pressure by a vacuum pump through which desorbed CO₂ and H₂O vapor were exhausted to the atmosphere. The outlet concentration of the liquid leaving the tower, i.e. the inlet concentration of the test column was about 0.008–0.015 g mole/l, which is much higher than the equilibrium value at this pressure and room temperature. By locating the tower at the highest possible elevation in the laboratory, 3 m above the floor where the circulating pumps were installed, smooth pump operation without cavitation was obtained. The stainless steel centrifugal pumps had magnetically driven impellers in order to eliminate contamination or leakage problems. The rotameter was calibrated with tap water and an ethylene glycol-water mixture and agreement found with the manufacturer's density correction formula. The filter was made by filling a 1-l three mouth flask with activated carbon pellets; the filter served to remove organic contaminants in the circulating liquid and it was found that the gas absorption rate decreased significantly when the carbon filter was not in use. The liquid temperature was controlled by a heating tape and a single pass heat exchanger with a refrigerant supply. The valves on all liquid lines were contamination free forged bonnet valves (Whitey Co. GNB58-316).

The gas flow was provided by a rotary blower with special features to eliminate gas contamination (Gardner—Denver Co., Model 2PDR4); gas flow rate was controlled with a by-pass valve system. The gas temperature was controlled by a heating tape wound on a copper line. A positive displacement flow-meter (Rockwell Model 415 test meter) was used for accurate gas flow rate measurement. Depending on whether co-current or counter-current operation of the test column was desired, the gas line was connected to the top or bottom of the test column; for absorption from a stagnant gas the gas loop was completely separated from the system.

2.2. Procedures

2.2.1. Preparation of system and test liquids. Special effort was required to maintain the system free of contamination and leakage. All components were cleaned thoroughly before assembly. The activated carbon in the liquid filter was rinsed in flowing tap water and distilled water for two days to leach out base ions. The base producing compounds were reduced to a level low

enough to ensure no effect on titration process used to measure CO₂ concentration. The ethylene glycol was of reagent grade (purity of 98 per cent by mole) and was mixed with distilled water to obtain the ethylene glycol-water mixtures. The density, viscosity, surface tension, CO₂ solubility and CO₂ molecular diffusivity were measured by the techniques described in [6] and are given in Table 1. The measured values compared well with those published by Hayduk [7].

2.2.2. Absorption from a stagnant gas. The test liquids were tap water at 14, 25 and 40°C, and ethylene glycol-water mixtures with glycol mole fractions of $X = 0.0, 0.522, 0.12$ and 0.20 . After leak testing and evacuating the system it was purged three times with CO₂. Foreign gases in the liquid were desorbed by running the system for about twenty minutes and any air remaining in the test section was purged by continuously flowing excess CO₂. The CO₂ supply was saturated with the test liquid by a bubbler before entering the column. The pressure in the test section was maintained at about 10 cm H₂O above ambient pressure. The temperature of the liquid was maintained within $\pm 0.2^\circ\text{C}$ of the desired value; for the tests with tap water at 14°C and 40°C the column was thermally insulated to maintain isothermal conditions.

It was found that inlet and outlet concentrations reached a steady state after about five passes and data was taken after ten to twenty passes. The sample solutions were drawn from the inlet and outlet sampling ports using two 50 cm³ hypodermic syringes; usually 25 cm³ of solution was used for titration. When testing tap water the inlet concentration was only measured once and there was no need to wait for system steady state. CO₂ gas was always supplied in excess to purge, as well as to minimize drag effects.

2.2.3. Absorption from co- and counter-current gas flows. With co-current gas flow the test liquids were tap water and two ethylene glycol-water mixtures ($X = 0.052, 0.12$) both at 25°C. With counter-current gas flow only tap water at 25°C was used. The gas flow loop was purged of air with CO₂ as described in the previous section. Sample gas was tested and titration showed the mole fraction of CO₂ in the gas flow loop, excluding water vapor, was 98–99 per cent. During operation the entire gas flow loop was maintained above atmospheric pressure to eliminate air leakage. The pressure drop along the test column was measured

using vertical and inclined manometers. The pressure in the test section for calculating the interfacial CO_2 concentration was calculated by subtracting one half the pressure drop from the column inlet pressure.

The liquid flow rate was held constant to give a desired Reynolds number, and the gas flow rate increased step by step from one run to another. The gas flow rate in the co-current flow experiments was increased up to the maximum capacity of the blower, while in the counter-current experiments the gas flow rate was severely limited by liquid hold-up choking the test column. A larger diameter column would be required to obtain counter-current data at higher gas velocities.

2.3. Calculation methods

The mass-transfer coefficient K_L was calculated from the measured experimental data and system parameters using

$$K_L = \frac{\Gamma}{\rho L} \frac{R}{R - \delta} \ln \frac{c_i - c_{in}}{c_i - c_{out}} \quad (3)$$

where c_i is the interfacial concentration of CO_2 , and c_{in} and c_{out} are the bulk concentrations at the inlet and outlet of the column, respectively. Equation (3) assumes that K_L is independent of z and that δ is uniform. In a turbulent falling film the species concentration profile becomes fully developed within a short distance of the inlet [8], so that the entrance effect on K_L is justifiably neglected for the length of test section used in the present study. The second mentioned assumption is clearly not realistic and consequently K_L calculated from equation (3) is an apparent or superficial coefficient which contains the effect of the increased transfer area.

The mean film thickness δ was calculated from the Brotz equation [9],

$$\delta^0 = 0.0672(v^2/g)^{1/3} Re_L^{2/3}. \quad (4)$$

The interfacial concentration of CO_2 , c_i , was calculated from Henry's law,

$$c_i = P_{\text{CO}_2}/H \quad (5)$$

where P_{CO_2} was taken to be equal to the bulk gas stream value. The Henry's law constant was calculated from the results of the solubility measurements reported in [6]. Two assumptions are so introduced. Firstly, the interfacial resistance is taken to be negligible owing to the relatively low mass transfer rate and the remote possibility that the accommodation coefficient is significantly below unity. Secondly, the gas-side resistance is taken to be negligible. Since the H_2O vapor in the CO_2 can condense the gas phase transport problem is complex; it is shown in [6] that the gas phase resistance is negligible under the conditions of the experiments.

The CO_2 concentrations c_{in} and c_{out} were determined using a common wet chemistry technique. The CO_2 in the liquid sample was precipitated as barium carbonate from a sodium hydroxide and barium chloride

solution, and the excess sodium hydroxide was titrated to the phenolphthalein end point with standardized hydrochloric acid. The concentration of the solutions used was about 0.1 M, and the barium chloride and sodium hydroxide solutions were used in 20–50 per cent excess. Great care was taken to isolate the solutions from ambient air.

The liquid side Reynolds number was defined by

$$Re_L = 4\Gamma/\rho v \quad (6)$$

and the superficial gas velocity V_g was calculated based on the column cross-sectional area. The interfacial shear was calculated from

$$\tau_i = \frac{R - \delta^0}{2} \left(\frac{dP}{dz} + \rho_g g \right). \quad (7)$$

The value in parentheses in equation (7) was calculated by dividing the water level difference in the differential manometer by the distance between the two pitot tubes (156 cm). In using δ^0 in equation (7) the thinning or thickening due to gas drag was ignored.

3. RESULTS AND DISCUSSION

3.1. Absorption from a stagnant gas

A comparison of the mass-transfer coefficient with zero interfacial shear, K_L^0 , obtained for distilled water at 25°C with the results of previous workers is shown in Fig. 2. The present values of K_L^0 are higher than those of Lamourelle and Sandall [5] and of Kamei and Oishi [2] except at the highest Reynolds numbers tested. Thus the corresponding Reynolds number power dependence of 0.67 found in the present work is appreciably lower than the 0.839 of [5] and a little lower than the 0.7 of [2]. Possible reasons for the discrepancy are (i) contamination of the water, (ii) differences in geometry (in [5] the film was on the outside wall of a 0.95 cm OD stainless steel tube; in [2] it was on the inside wall of a 5.1 cm OD glass pipe), and (iii) errors in liquid flow rate measurement. The most likely of these three reasons is the contamination problem. In the present study lower values of K_L^0 were obtained when the water was recycled without the charcoal filter in the loop; it was only after high values of K_L^0 were obtained for once-through tap water operation that the importance of complete elimination of contamination was fully appreciated. In [5] the water was

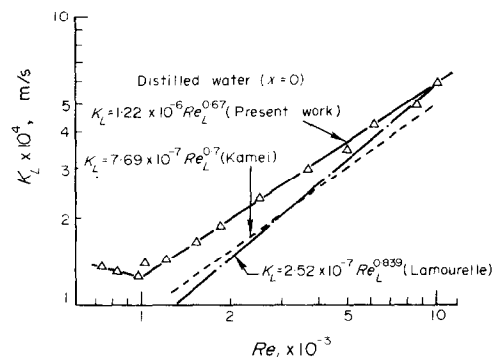


FIG. 2. Comparison of K_L^0 vs Re_L for distilled water at 25°C with other workers.

Table 2. Values of a and n in $K_L^0 = aRe_L^n$, and b in $K_L^0/\mathcal{D}(v^2/g)^{1/3} = bRe_L^n Sc^{1/2}$

X	$a \times 10^7$ (m/s)	$b \times 10^4$	n
Ethylene glycol-water mixtures at 25°C			
0.0	12.2	12.7	0.67
0.052	4.0	4.9	0.81
0.12	1.20	1.69	0.94
0.20	0.224	0.39	1.14
Tap water			
$T^\circ\text{C}$			
40	29.6	24.4	0.568
25	15.2	15.7	0.63
14	6.52	8.2	0.717

recycled and no mention is made of a filter in the liquid loop. In this regard the experiments of Orridge [10] are pertinent. In that work gas absorption into a film flowing over a roughened inclined plate was measured for various concentrations of added surfactant; only 0.1 ppm surfactant was found to reduce K_L^0 by 15 per cent. A contamination level of 0.1 ppm is very low, but is detectable by the Crits ring test [11]. In the present study the Crits ring test was used to monitor water purity, but the previous workers make no mention of such precautionary measures.

The results for the three ethylene glycol-water mixtures are shown in Fig. 3. It can be seen the Reynolds number power dependence increases with concentration of ethylene glycol. An examination of the property values in Table 1 shows that only viscosity varies appreciably with concentration so that it is suggested that the Reynolds number power dependence depends essentially on viscosity, a result which is confirmed by the tap water results. The maximum Reynolds number for the highest viscosity liquid ($X = 0.2$) was limited to about 4000 by the capacity of the rotameter. The Reynolds number for transition from wavy laminar to turbulent flow can be clearly seen in Fig. 3; it is also evident that K_L^0 is nearly constant in the wavy

laminar regime, in marked contrast to the trend seen in the turbulent regime. This feature is due to the common driving force expression used to define K_L^0 in both regimes, $K_L^0 = N_A/(c_i - c_b)$. This definition is appropriate for the turbulent regime where the steep concentration profile ensures a value of c at the "edge" of the concentration boundary-layer close to c_b . On the other hand, in the wavy laminar regime at short contact times the value of c at the edge of the concentration boundary layer is c_{in} , and the thicker concentration boundary layer gives $c_b > c_{in}$. The use of $(c_i - c_{in})$ as the driving force in the wavy laminar regime would give lower values of K_L^0 and a monotonic increase in K_L^0 with Re_L . Of course, N_A itself increases monotonically with Re_L .

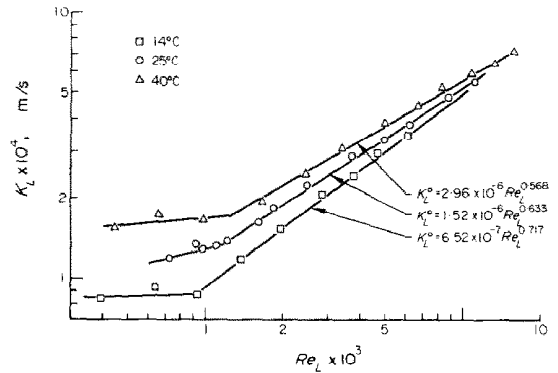


FIG. 4. K_L^0 vs Re_L for tap water at 14, 25 and 40°C.

The results for tap water at 14, 25 and 40°C are shown in Fig. 4. Again, reference to Table 1 shows that the density and surface tension of these liquids do not differ by much, but there is a factor of two decrease in viscosity. As was the case for the ethylene glycol mixtures, the Reynolds number power dependence is seen to increase with viscosity. Kamei and Oishi [2] also tested water at different temperatures but the scatter in their data is such that this Reynolds number power dependence trend was not discernible.

In view of the well established approximately one-half power dependence of K_L^0 on molecular diffusivity, the data is replotted as $K_L^0/\mathcal{D}^{1/2}$ vs Re_L in Fig. 5. However for correlation purposes a dimensionless representation is desirable. Dimensional analysis of the problem of gas absorption into a turbulent falling film suggests the following as a complete set of dimensionless products:

$$K_L^0/(g\nu)^{1/3}; Re_L; \nu(g\rho^3/\sigma^3)^{1/4}; Sc$$

where the third product above is a physical properties group sometimes called the capillary-buoyancy number. In view of the observed power law dependence on Re_L and the previously established one-half power dependence on \mathcal{D} a correlation of the form

$$\frac{K_L^0}{(g\nu)^{1/3}} = Re_L^n Sc^{-1/2} f\{\nu(g\rho^3/\sigma^3)^{1/4}\} \quad (8)$$

is suggested, and the function f is shown in Fig. 6. Two

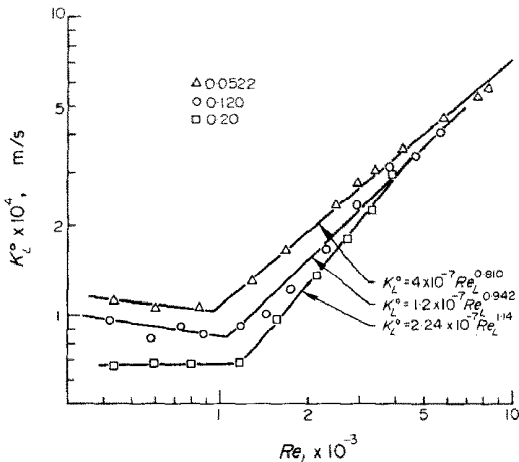


FIG. 3. K_L^0 vs Re_L for ethylene glycol-water mixtures at 25°C with glycol mole fractions of 0.0522, 0.12 and 0.20.

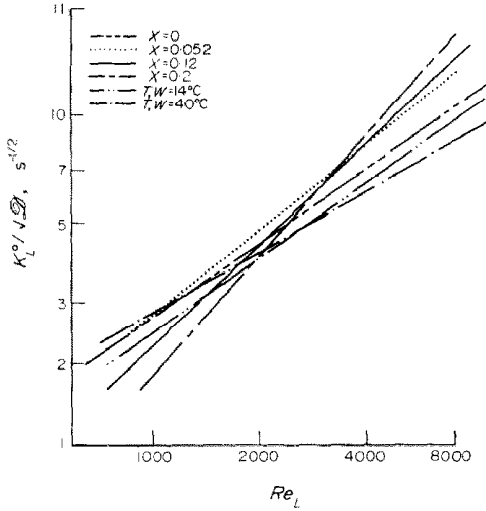


FIG. 5. Comparison of $K_L^0/\sqrt{\gamma}$ vs Re_L for six liquids used in the zero interfacial shear experiments.

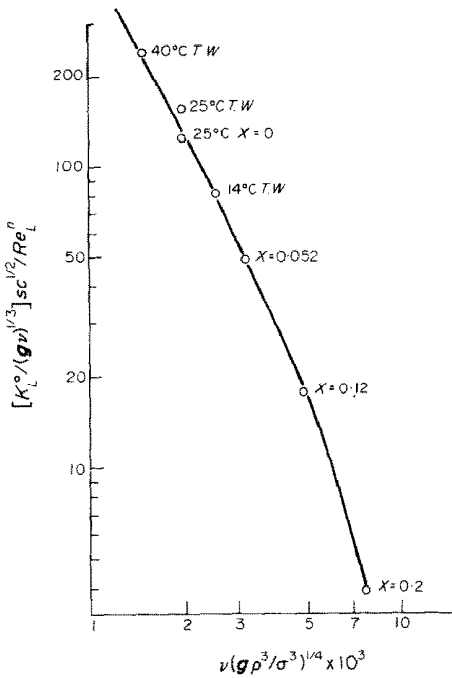


FIG. 6. Empirical correlation of K_L^0 as $[K_L^0/(g v)^{1/3}] Sc^{1/2}/Re_L^0$ vs $v(g \rho^3/\sigma^3)^{1/4}$ for seven liquids.

correlations of the Reynolds number exponent n are shown in Figs. 7. In Fig. 7(a) n is correlated simply as a function of kinematic viscosity ν , and in Fig. 7(b) as a function of the dimensionless groups Sc and $v(g \rho^3/\sigma^3)^{1/4}$. Both are satisfactory for engineering use. Correlations of n with Sc or $v(g \rho^3/\sigma^3)^{1/4}$ alone were found to be markedly inferior. Table 2 shows values of a and n in data fits of the form $K_L^0 = a Re_L^n$, and $(K_L^0/\mathcal{D})(v^2/g)^{1/3} = b Re_L^n Sc^{1/2}$. The two correlations for n are

$$n = 6.95 \times 10^{-2} (\nu \text{ m}^2/\text{s})^{1/2} \quad (9)$$

or

$$n = 2.08 Sc^{0.095} \{v(g \rho^3/\sigma^3)^{1/4}\}^{0.277} \quad (10)$$

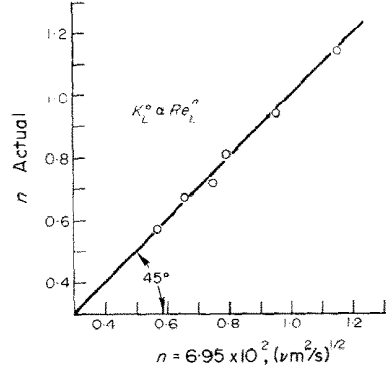


FIG. 7(a). Empirical correlation of Reynolds number power dependence with kinematic viscosity for seven liquids.

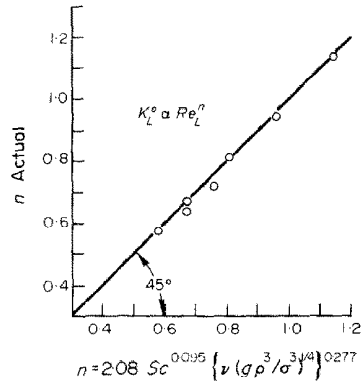


FIG. 7(b). Empirical correlation of Reynolds number power dependence with dimensionless groups Sc and $v(g \rho^3/\sigma^3)^{1/4}$ for seven liquids.

3.2. Transition Reynolds number

Figures 2–5 show that the transition from wavy laminar to turbulent flow occurs rather sharply at Reynolds numbers of 1000–1200. The transition Reynolds numbers obtained from these figures, together with values obtained from other sources are listed in Table 3. Kamei and Oishi's values [2] were obtained from gas absorption measurements, while Chun and Seban [12] measured heat transfer across a falling film with surface evaporation. Chun and Seban suggested that a Weber number of unity might be a reasonable criterion for transition from wavy laminar to turbulent flow; in the bottom row of Table 3 are the Weber numbers corresponding to the transition Reynolds numbers obtained in the present work. Here Weber number is defined by $We^2 = \rho_L u_b^2/\sigma$ with u_b calculated from Nusselt laminar flow theory.

Table 3 shows that while Weber number for water at different temperatures is constant and close to unity, for ethylene glycol mixtures of high viscosity the transition Weber numbers are appreciably larger than unity. Clearly Table 3 shows that, for the liquids tested, Reynolds number is the superior criterion for transition. We also note that for co-current gas flow the transition has been found to occur at lower Reynolds numbers [13], but a study of the effect of gas velocity on transition was not part of the present experimental program.

Table 3. Reynolds numbers for transition from wavy laminar to turbulent film flow

	Ethylene glycol–water mixture				Tap water		
	$X = 0.0$	$X = 0.02$	$X = 0.12$	$X = 0.2$	40°C	25°C	14°C
Present work	1100	960	1050	1150	1200	1140	1050
Kamei and Oishi [2]	—	—	—	—	2000	2000	2000
Chun and Seban [12]	—	—	—	—	1150	900	820
Weber number	1.44	1.43	2.90	3.63	1.41	1.46	1.47

3.3. Absorption from co- and counter-current gas flows

With co-current gas flow the gas velocity ranged from 0 to about 14 m/s. According to Hewitt and Hall-Taylor [14] the onset of liquid entrainment for this geometry occurs at a gas velocity of about 10 m/s so most of the data is for the pure annular flow regime. A marked increase in K_L due to interfacial shear was found. Figure 8 shows the results for tap water at 25°C plotted in the normalized form K_L/K_L^0 vs τ_i/τ_w^0 where τ_i is the interfacial shear stress calculated from pressure drop

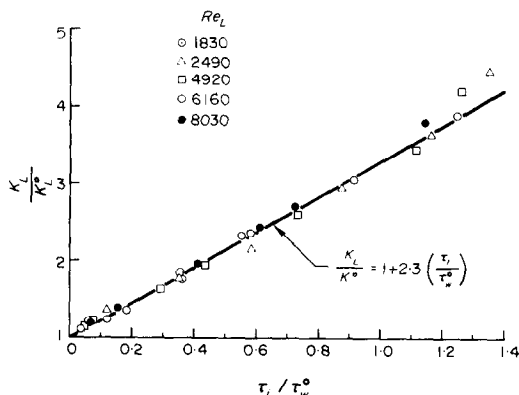


FIG. 8. Normalized plot of K_L as a function of τ_i for co-current tap water at 25°C.

measurements using equation (7), and τ_w^0 is the wall shear stress at zero gas velocity [$\tau_w^0 = \rho g \delta^0$ with δ^0 calculated from equation (4)]. In this form the data are well correlated by a simple linear relationship,

$$\frac{K_L}{K_L^0} = 1 + 2.3 \frac{\tau_i}{\tau_w^0} \quad (11)$$

for Re_L in the range 1830–8030. The marked increase in K_L with increasing gas velocity is attributed to more intensive turbulent mixing in the liquid phase near the interface due to vorticity generated by the interfacial shear. An attempt was made to theoretically predict the effect of interfacial shear on the mass-transfer coefficient using an eddy diffusivity model, but the results were disappointing and the work will not be reported here.

The results for co-current gas flow with ethylene glycol–water mixture of $X = 0.12$ are shown in normalized form in Fig. 9. These data are also well correlated by a linear relationship

$$\frac{K_L}{K_L^0} = 1 + 7.0 \frac{\tau_i}{\tau_w^0} \quad (12)$$

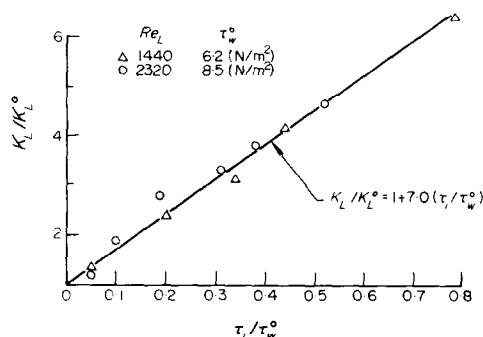


FIG. 9. Normalized plot of K_L as a function of τ_i for co-current flow of ethylene glycol–water mixture ($X = 0.12$).

For a Reynolds number of 2320 equation (11) reduces to

$$\frac{K_L}{K_L^0} = 1 + 0.460\tau_i(\text{N/m}^2) \quad (13)$$

while equation (12) reduces to

$$\frac{K_L}{K_L^0} = 1 + 0.824\tau_i(\text{N/m}^2). \quad (14)$$

Thus it is seen that the effect of interfacial shear on K_L is greater for the ethylene glycol mixture than for tap water. The significant difference between the two liquids is their viscosities and hence the Schmidt numbers, 1540 for the glycol mixture vs 485 for water. Thus the concentration boundary layer will be thinner for the glycol mixture, and hence more sensitive to the changes in turbulent mixing near the interface induced by interfacial shear.

In order to develop a correlation for the constant of proportionality in the relation

$$\frac{K_L}{K_L^0} = 1 + \alpha \frac{\tau_i}{\tau_w^0} \quad (15)$$

a liquid of intermediate viscosity, ethylene glycol–water mixture of $X = 0.052$, was tested. The results are shown in Fig. 10 where again the linearity is good, and $\alpha = 3.8$. The coefficient α for the three liquids was correlated as a function of liquid kinematic viscosity to give

$$\alpha = 0.9 + 1.73 \times 10^{12}(\text{vm}^2/\text{s})^2. \quad (16)$$

A limited amount of data were obtained for gas absorption into tap water with counter-current gas flow. In Fig. 11 the results are shown in normalized form K_L/K_L^0 vs τ_i/τ_w^0 . It is seen that, in contrast to the situation for co-current gas flow, the normalization

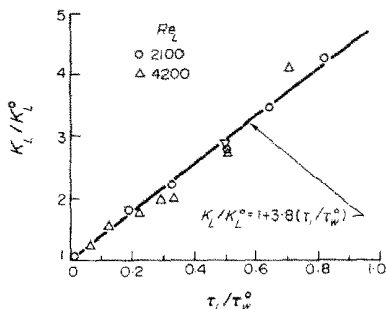


FIG. 10. Normalized plot of K_L as a function of τ_i for co-current flow of ethylene glycol-water mixture ($X = 0.052$).

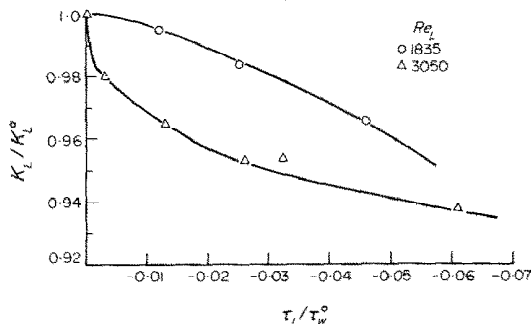


FIG. 11. Normalized plot of K_L as a function of τ_i for counter-current flow of tap water at 25°C.

does not remove Re_L as a parameter, nor is there a simple linear relationship. As expected counter-current gas flow does reduce the mass transfer coefficient. The gas velocity was restricted to a relatively low value (0.3 m/s) owing to aforementioned liquid hold-up problem. No quantitative conclusion is attempted due to the limited data.

4. CONCLUSIONS

1. For absorption from a stagnant gas into distilled water at 25°C the mass-transfer coefficients obtained were generally higher than those found in previous studies, and were correlated as

$$K_L = 1.22 \times 10^{-6} Re_L^{0.67} \text{ m/s.}$$

2. The mass-transfer coefficient for seven test liquids could be correlated as

$$\frac{K_L^0}{(\nu g)^{1/3}} = Re_L^n Sc^{-1/2} f\{\nu(g\rho^3/\sigma^3)^{1/4}\}$$

where the Reynolds number exponent n increased with viscosity and was correlated as

$$n = 2.08 Sc^{0.095} \{\nu(g\rho^3/\sigma^3)^{1/4}\}^{0.277}$$

and f is a graphed function.

3. The Reynolds number for transition from wavy laminar to turbulent flow ranged from 1000 to 1200; a criterion based on Weber number proved to be inappropriate.

4. With co-current gas flow interfacial shear resulted in a marked increase in K_L ; this effect increased with Schmidt number. For tap water and ethylene glycol-water mixtures K_L could be conveniently correlated by a linear relationship of the form

$$K_L/K_L^0 = 1 + \alpha(\tau_i/\tau_w^0)$$

$$\alpha = 0.9 + 1.73 \times 10^{12} (\text{m}^2/\text{s})^2.$$

5. With counter-current gas flow at low velocities K_L decreased with increasing gas velocity.

REFERENCES

1. L. E. Scriven, Flow and transfer at fluid interface, *Chem. Engng Educ.* **3**, Fall, 150–155 (1968) and **4**, Winter, 26–29 (1969).
2. S. Kamei and J. Oishi, Mass and heat transfer in a falling liquid film of wetted tower, *Mem. Fac. Kyoto Univ.* **17**, 229–289 (1955).
3. R. E. Emmert and R. L. Pigford, A study of gas absorption in falling liquid films, *Chem. Engng Prog.* **50**, 87–93 (1954).
4. J. T. Davies and K. V. Warner, The effect of large-scale roughness in promoting gas absorption, *Chem. Engng Sci.* **24**, 231–240 (1969).
5. A. P. Lamourelle and O. C. Sandall, Gas absorption into a turbulent liquid, *Chem. Engng Sci.* **27**, 1035–1042 (1972).
6. D. K. Chung, An experimental investigation of gas absorption into a turbulent liquid film with interfacial shear, Ph.D. Dissertation, School of Engineering and Applied Science, University of California, Los Angeles (1974).
7. W. Hayduk and V. K. Malik, Density, viscosity, carbon dioxide solubility and diffusivity in aqueous ethylene glycol solutions, *J. Chem. Engng Data* **16**, 143–146 (1971).
8. C. J. King, Turbulent liquid phase mass transfer at a free gas-liquid interface, *Ind. Engng Chem.* **5**, 1–8 (1966).
9. W. Brötz, Über die Vorausberechnung der Absorptionsgeschwindigkeit von Gasen in Strömen der Flüssigkeitsschichten, *Chem. Engng Tech.* **26**, 470–478 (1954).
10. J. T. Davies, *Turbulence Phenomena*, p. 260. Academic Press, New York (1972).
11. G. J. Crits, A simple test for trace organic substances in water, Symposium on Analytic Methods with Emphasis on Minor Elements, American Chem. Soc. (September 1961).
12. K. R. Chun and R. A. Seban, Heat transfer to evaporating liquid films, *J. Heat Transfer* **93**, 391–396 (1971).
13. I. G. Shekrladze, S. H. A. Mestvirishvili and A. N. Mikashvidze, Experimental study of the effect of condensation on transition to turbulent flow in a descending liquid film with co-current gas flow, *Heat Transfer—Soviet Res.* **3**, 120–122 (1971).
14. G. F. Hewitt and N. S. Hall-Taylor, *Annular Two-Phase Flow*, p. 136. Pergamon Press, Oxford (1970).

ETUDE EXPERIMENTALE DE L'ABSORPTION DE GAZ DANS DES FILMS TURBULENTS TOMBANTS D'EAU ET DE MELANGES D'EAU ET D'ETHYLENE-GLYCOL

Résumé—Des expériences sont présentées sur l'effet de la viscosité du liquide et du cisaillement à l'interface sur le coefficient de transfert de masse côté liquide dans l'écoulement en film turbulent. Le gaz carbonique était absorbé par un film liquide formé sur la paroi interne d'une tube vertical de diamètre intérieur 2,05 cm et de longueur 1,98 m. Il a été trouvé que la loi puissance qui fixe la dépendance du coefficient de transfert de masse sur le nombre de Reynolds dépend fortement de la viscosité. La transition

entre le mouvement laminaire ondulatoire et le mouvement turbulent se situe à des nombres de Reynolds allant de 100 à 1200. Dans le cas d'un écoulement de gaz dans le même sens, une augmentation linéaire très marquée du coefficient de transfert de masse est trouvée, tandis que dans le cas d'un écoulement de gaz à contre-courant le coefficient diminue.

EXPERIMENTELLE UNTERSUCHUNG EINES TURBULENTEN RIESELFILMS AUS WASSER UND GLYKOL-WASSER-MISCHUNGEN

Zusammenfassung—Es wird über Untersuchungen des Einflusses der Viskosität der Flüssigkeit und der Scherkräfte an der Phasengrenzfläche auf den Stoffübergangskoeffizienten auf der Flüssigkeitsseite eines turbulenten Rieselfilms berichtet. Gasförmiges CO_2 wurde von einem Rieselfilm, der an der Innenseite eines vertikalen Rohres (Innendurchmesser 20,5 mm, Länge 1,98 m) herabströmte, absorbiert. Der Exponent der Reynolds-Zahl zur Bestimmung des Stoffübergangskoeffizienten ist stark abhängig von der Viskosität. Der Übergang vom wellig laminaren zum turbulenten Rieselfilm stellte sich bei einer Reynolds-Zahl von 1000 bis 1200 ein. Bei Gegenstrom von Gas und Rieselfilm wurde ein deutlicher und linearer Anstieg des Stoffübergangskoeffizienten festgestellt, während sich dieser bei Gleichstrom verringerte.

ЭКСПЕРИМЕНТАЛЬНОЕ ИССЛЕДОВАНИЕ ГАЗОПОГЛОЩЕНИЯ ТУРБУЛЕНТНЫМИ ПАДАЮЩИМИ ПЛЕНКАМИ ВОДЫ И ЭТИЛЕНГЛИКОЛЬ-ВОДНЫМИ СМЕСЯМИ

Аннотация — Приводятся экспериментальные результаты по эффектам влияния вязкости жидкости и межфазного сдвига на коэффициент массопереноса жидкости для турбулентных падающих пленок. Углекислый газ поглощался жидкой пленкой, образованной внутри вертикальной трубы с внутренним диаметром 2,05 см и длиной 1,98 м. Найдено, что степенная зависимость коэффициента массопереноса от числа Рейнольдса сильно зависит от вязкости. Переход от волнистого ламинарного к турбулентному потоку имел место при числах Рейнольдса от 1000 до 1200. При спутном потоке газа обнаружено значительное линейное увеличение коэффициента массопереноса, в то время как этот же коэффициент уменьшается при течении газа в противоположном направлении.